

Line tension from dual-geometry sessile droplet measurements: Combining contact angle size dependence data for axisymmetric and cylindrical droplets to determine the line tension

Dmitry V. Tatyanyenko* and Konstantin D. Apitsin

Department of Statistical Physics, Faculty of Physics, Saint Petersburg State University
7–9 Universitetskaya nab., St. Petersburg, 199034, Russia

(Dated: August 2, 2024)

We perform a thermodynamic analysis of various contributions to the size dependence of the contact angle cosine for axisymmetric and cylindrical sessile droplets. This shows that a widely used method to determine the line tension from the slope of the contact angle cosine dependence on the three-phase contact line curvature (for axisymmetric droplets) provides a certain combination of the line tension, adsorptions at the three interfaces, and the macroscopic contact angle. To extract the leading-order contact-line-related contribution and determine the line tension, we propose a simple technique using contact angle size dependences for axisymmetric and cylindrical droplets at the same conditions.

I. INTRODUCTION

The contact angle of a large sessile droplet can be found from the well-known classical Young equation [1]

$$\sigma^{\alpha\beta} \cos \theta_\infty = \sigma^{\beta\gamma} - \sigma^{\alpha\gamma} \quad (1)$$

with σ the surface tension of a corresponding interface, θ_∞ the macroscopic contact angle; α , β , and γ mark the liquid, gaseous and solid phases, respectively, and double Greek superscripts mark the corresponding interfaces. The surface tensions here are thermodynamic (defined as the surface excesses of the grand potential per unit area of the interface). For small droplets, the thermodynamic line tension κ (defined as the line excess of the grand potential per unit length of the three-phase contact line [2, 3]) affects the contact angle [3–9]:

$$\sigma^{\alpha\beta} \cos \theta_a = \sigma^{\beta\gamma} - \sigma^{\alpha\gamma} - \frac{\kappa}{r_a}. \quad (2)$$

Here θ is the contact angle, r is the radius of the three-phase contact line, subscript “a” refers to axisymmetric droplet (see Fig. 1(a)); the line tension κ is implied to be constant. Eq. (2) is usually called the modified Young equation.

Subtracting the modified Young equation (2) from the classical one (1) and dividing the both parts of the resulting equation by $\sigma^{\alpha\beta}$, one usually arrives at [3, 5, 7, 8]

$$\cos \theta_\infty - \cos \theta_a = \frac{\kappa}{\sigma^{\alpha\beta} r_a}. \quad (3)$$

This equation is widely used for contact-angle-based measurements of the line tension in laboratory experiments (see, e.g., [10]) and computer modeling (e.g., molecular dynamics simulations [11–20]). According to Eq. (3), the slope of the graph $\cos \theta_a$ vs $1/r_a$ must be equal to $-\kappa/\sigma^{\alpha\beta}$. The surface tension $\sigma^{\alpha\beta}$ is typically measured or calculated separately.

However, some authors have noted that Eq. (3) is generally not correct [21–24], since it assumes the corresponding surface tensions in Eqs. (1) and (2) to be equal, whereas they correspond to different equilibrium sessile droplet sizes, which

implies different values of the chemical potential(s). There are arguments that adsorption at the solid–liquid interface and its effect on the surface tension $\sigma^{\alpha\gamma}$ affect $\cos \theta_a$ in the same manner and with a similar magnitude as it is measured in experiments [25], so the line tension itself is not necessary to explain the dependence of $\cos \theta_a$ on $1/r_a$. Consideration with use of an interface displacement model shows [21] that the contributions of the line tension and the adsorption at the solid–gas interface (and its effect on the surface tension $\sigma^{\beta\gamma}$) to the dependence of $\cos \theta_a$ on $1/r_a$ can be comparable in the presence of a precursor film. Some authors [18, 26] suppose only $\sigma^{\alpha\beta}$ to depend on the droplet size and Eq. (3) to be correct, but the slope of the graph $\cos \theta_a$ vs $1/r_a$ to give a quantity not equal to $-\kappa/\sigma^{\alpha\beta}$. Sometimes the resulting “line tension” is called the *apparent* line tension [20, 22, 26–30]. General thermodynamic analysis shows [21, 24] that the value of this slope has contributions both from the line tension and the adsorptions at all three interfaces (see also [31] for similar arguments).

How to “extract” the line-tension contribution and determine the value of the line tension from the measurements or calculations of $\cos \theta$ vs $1/r$? Thermodynamic analysis shows [24] that, for cylindrical droplets [long liquid “channels”, or “filaments”, or “ridges” attached to the substrate surface, see Fig. 1(b)], there is no κ/r term in the equation corresponding to (2). It means that dependence of the contact angle θ_c on the size of a cylindrical droplet (e. g., its half-width r_c on the substrate) is governed by dependences of the surface ten-

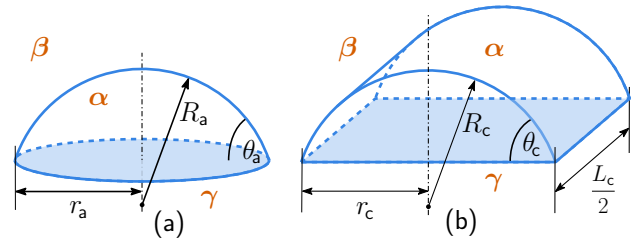


Figure 1. Axisymmetric (a) and cylindrical (b) sessile droplets. R is the curvature radius of the liquid–gas interface, θ is the contact angle, r is the radius (half-width) of the droplet on the substrate. Subscript “a” marks quantities for axisymmetric, “c” — for cylindrical droplets. Phases: α — liquid, β — gas (vapor), γ — solid substrate.

* d.tatyanyenko@spbu.ru

sions and the droplet size on the chemical potential(s). This suggests the idea to compare or combine data of size dependence of $\cos \theta$ for axisymmetric and cylindrical droplets at the same conditions to exclude the surface-tension-related contributions and determine the line tension.

In section II, we present a thermodynamic analysis of various contributions to droplet size dependence of the contact angle for both axisymmetric and cylindrical droplets in a system with a single-component fluid and an ideal smooth homogeneous solid substrate in absence of external fields. Based on it, in section III we propose a simple technique that allows to determine the line tension from a combination of contact angle size dependences for axisymmetric and cylindrical droplets in a manner similar to use of Eq. (3).

Cylindrical droplets are often used in modeling, e.g., in molecular dynamics (MD) simulations [14, 15, 18, 20, 22, 32–37] due to convenient use of periodic boundary conditions along their longitudinal axes and due to expected independence of the contact angle of (or a weak dependence on) the droplet width. However, they are hardly available for experimental measurements due to Plateau–Rayleigh-type instability [38]. Thus, the technique we propose is mainly oriented to modeling, especially with methods not allowing for direct calculation of the line excess of the grand potential (e.g., MD simulations). The dimensions of such simulated axisymmetric and cylindrical droplets, i.e., R , r , and θ , can be “measured”, and these data can be used to determine the line tension.

II. THERMODYNAMICS AND CONTACT ANGLES

A. Equilibrium conditions for sessile droplets

For thermodynamic description of a small sessile droplet on a partially wettable substrate, we consider a materially open system of a fixed volume including the droplet itself, the substrate, and the surrounding gas (vapor). The liquid and gaseous phases are supposed to be a single-component fluid at a given values of chemical potential μ and temperature T (that supposed to be constant). The grand thermodynamic potential of the system decomposes into bulk, surface, and line parts:

$$\Omega = -p^\alpha V^\alpha - p^\beta V^\beta + \omega^\gamma V^\gamma + \sigma^{\alpha\beta} A^{\alpha\beta} + \sigma^{\alpha\gamma} A^{\alpha\gamma} + \sigma^{\beta\gamma} A^{\beta\gamma} + \kappa L \quad (4)$$

with V the volume, A the area of the interface, L the length of the three-phase contact line, p the pressure in the bulk phase, ω the bulk density of the grand thermodynamic potential (in fluid phases equals $-p$). Other quantities as well as notations of phases and interfaces has been explained above.

Let us consider two types of droplet geometry: (1) axisymmetric droplet [shaped as a spherical segment in our “macroscopic” thermodynamic description, see Fig. 1(a)] and (2) a fixed-length piece of a cylindrical droplet [shaped as a segment of a circular cylinder in our “macroscopic” thermodynamic description, see Fig. 1(b)]. In both geometries, the cross-section of the droplet in our “macroscopic” thermody-

amic description is a circular segment, therefore,

$$r = R \sin \theta. \quad (5)$$

Thus, the shape and size of the droplet can be described by two independent variables, e.g., (R, r) , (R, θ) or (r, θ) .

In both geometries, choosing the $\alpha\beta$ dividing surface to be the surface of tension, one can obtain equilibrium conditions for sessile droplets by expressing all the volumes, areas and the length of the three-phase contact line in (4), and solving one of the following sets of two equations

$$\partial\Omega(R, r, T, \mu)/\partial R = 0 \quad \text{and} \quad \partial\Omega(R, r, T, \mu)/\partial r = 0, \quad (6a)$$

$$\partial\Omega(R, \theta, T, \mu)/\partial R = 0 \quad \text{and} \quad \partial\Omega(R, \theta, T, \mu)/\partial \theta = 0, \quad (6b)$$

$$\partial\Omega(r, \theta, T, \mu)/\partial r = 0 \quad \text{and} \quad \partial\Omega(r, \theta, T, \mu)/\partial \theta = 0, \quad (6c)$$

and then taking into account the geometric relation (5). Since T and μ are constant, the pressures and the surface tensions in (4) will be constant at such variations (for $\sigma^{\alpha\beta}$, this also requires $\partial\sigma^{\alpha\beta}/\partial R = 0$ which is true namely for the surface of tension chosen as the $\alpha\beta$ dividing surface).

The droplet-size-dependent surface tensions $\sigma_a^{\alpha\beta}$ and $\sigma_c^{\alpha\beta}$ for spherical and cylindrical interfaces can generally differ, though their difference is expected to be very small at the same value of μ (see subsection II B).

Let us chose R and θ as independent variables describing the sessile droplet. Introducing non-variable quantities for the total volume occupied by the fluid $V_t \equiv V^\alpha + V^\beta$ and the total area of the substrate $A_t \equiv A^{\alpha\gamma} + A^{\beta\gamma}$ and using relation (5), one can express the volumes, areas, and the contact line length for an axisymmetric droplet as

$$V_a^\alpha = \frac{\pi R_a^3}{3} (2 + \cos \theta_a) (1 - \cos \theta_a)^2, \quad L_a = 2\pi R_a \sin \theta_a,$$

$$A_a^{\alpha\beta} = 2\pi R_a^2 (1 - \cos \theta_a), \quad A_a^{\alpha\gamma} = \pi R_a^2 \sin^2 \theta_a,$$

$$V_a^\beta = V_t - V_a^\alpha, \quad A_a^{\beta\gamma} = A_t - A_a^{\alpha\gamma}.$$

Decomposition (4) of the grand potential then takes form

$$\begin{aligned} \Omega_a(R_a, \theta_a) = & -(p^\alpha - p^\beta) \frac{\pi R_a^3}{3} (2 + \cos \theta_a) (1 - \cos \theta_a)^2 \\ & + 2\pi \sigma_a^{\alpha\beta} R_a^2 (1 - \cos \theta_a) + (\sigma^{\alpha\gamma} - \sigma^{\beta\gamma}) \pi R_a^2 \sin^2 \theta_a \\ & + 2\pi \kappa_a R_a \sin \theta_a - p^\beta V_t - \sigma^{\beta\gamma} A_t. \end{aligned}$$

Application of the equilibrium conditions (6b) gives

$$\begin{aligned} & -\pi R_a^2 (p^\alpha - p^\beta) (2 + \cos \theta_a) (1 - \cos \theta_a)^2 \\ & + 4\pi R_a \sigma_a^{\alpha\beta} (1 - \cos \theta_a) + 2\pi R_a (\sigma^{\alpha\gamma} - \sigma^{\beta\gamma}) \sin^2 \theta_a \\ & + 2\pi \kappa_a \sin \theta_a + 2\pi R_a \frac{\partial \kappa_a}{\partial R_a} \sin^2 \theta_a = 0, \\ & -\pi R_a^3 (p^\alpha - p^\beta) \sin^3 \theta_a + 2\pi \sigma_a^{\alpha\beta} R_a^2 \sin \theta_a + 2\pi \kappa_a R_a \cos \theta_a \\ & + 2\pi R_a^2 (\sigma^{\alpha\gamma} - \sigma^{\beta\gamma}) \sin \theta_a \cos \theta_a + 2\pi R_a^2 \frac{\partial \kappa_a}{\partial R_a} \sin \theta_a \cos \theta_a = 0. \end{aligned}$$

To exclude the pressure difference $p^\alpha - p^\beta$, we multiply the first equation by $(2\pi R_a)^{-1} \sin^2 \theta_a (1 - \cos \theta_a)^{-2}$

and then subtract the second equation multiplied by $(2 + \cos \theta_a)(2\pi R_a^2 \sin \theta_a)^{-1}$ [39]. After some trigonometric simplifications and substitution of the result into one of the above equilibrium conditions, we arrive at the Laplace equation and the generalized Young equation as equilibrium conditions for an axisymmetric sessile droplet [3, 7, 8, 21, 24, 40]

$$p^\alpha - p^\beta = \frac{2\sigma_a^{\alpha\beta}}{R_a}, \quad (7)$$

$$\sigma_a^{\alpha\beta} \cos \theta_a = \sigma^{\beta\gamma} - \sigma^{\alpha\gamma} - \frac{\kappa_a}{r_a} - \frac{\partial \kappa_a}{\partial r_a} \quad (8)$$

For a cylindrical droplet,

$$\begin{aligned} V_c^\alpha &= \frac{L_c R_c^2}{4} (2\theta_c - \sin 2\theta_c), \\ A_c^{\alpha\beta} &= L_c R_c \theta_c, \quad A_c^{\alpha\gamma} = L_c R_c \sin \theta_c, \\ V_c^\beta &= V_t - V_c^\alpha, \quad A_c^{\beta\gamma} = A_t - A_c^{\alpha\gamma}, \end{aligned}$$

and the length L_c of the three-phase contact line does not depend on R_c and θ_c [see Fig. 1(b)] and supposed to be constant. Contact angle θ_c here is in radians. Decomposition (4) of the grand potential then takes form

$$\begin{aligned} \Omega_c(R_c, \theta_c) &= -(p^\alpha - p^\beta) \frac{L_c R_c^2}{4} (2\theta_c - \sin 2\theta_c) + \sigma_c^{\alpha\beta} L_c R_c \theta_c \\ &\quad + (\sigma^{\alpha\gamma} - \sigma^{\beta\gamma}) L_c R_c \sin \theta_c + \kappa_c L_c - p^\beta V_t - \sigma^{\beta\gamma} A_t. \end{aligned}$$

Application of the equilibrium conditions (6b) gives

$$\begin{aligned} &-(p^\alpha - p^\beta) L_c R_c (\theta_c - \sin \theta_c \cos \theta_c) + \sigma_c^{\alpha\beta} L_c \theta_c \\ &\quad + (\sigma^{\alpha\gamma} - \sigma^{\beta\gamma}) L_c \sin \theta_c + L_c \frac{\partial \kappa_c}{\partial r_c} \sin \theta_c = 0, \\ &-(p^\alpha - p^\beta) L_c R_c^2 \sin^2 \theta_c + \sigma_c^{\alpha\beta} L_c R_c \\ &\quad + (\sigma^{\alpha\gamma} - \sigma^{\beta\gamma}) L_c R_c \cos \theta_c + L_c R_c \frac{\partial \kappa_c}{\partial r_c} \cos \theta_c = 0. \end{aligned}$$

Here we have employed trigonometric equalities $\sin 2\theta_c = 2 \sin \theta_c \cos \theta_c$ and $1 - \cos 2\theta_c = 2 \sin^2 \theta_c$. To obtain a simpler equation for $p^\alpha - p^\beta$, we multiply the first equation by $R_c \cos \theta_c$ and subtract the second equation multiplied by $\sin \theta_c$. After some simplifications and substitution of the result into one of the above equilibrium conditions, we arrive at the Laplace equation and the generalized Young equation as equilibrium conditions for an cylindrical sessile droplet, slightly different from Eqs. (7) and (8):

$$p^\alpha - p^\beta = \frac{\sigma_c^{\alpha\beta}}{R_c}, \quad (9)$$

$$\sigma_c^{\alpha\beta} \cos \theta_c = \sigma^{\beta\gamma} - \sigma^{\alpha\gamma} - \frac{\partial \kappa_c}{\partial r_c}. \quad (10)$$

The absence of the coefficient 2 in the Laplace equation (9) for the cylindrical droplet can be explained by the fact that its $\alpha\beta$ interface is curved only along one direction, whereas the spherical droplet has equal curvatures along two directions.

The line-tension terms in the generalized Young equations (8) and (10) originate from variations of the line term κL in (4). For an axisymmetric droplet, $L_a = 2\pi r_a$ and $\partial(\kappa_a L_a)/\partial r_a = 2\pi \kappa_a + 2\pi r_a \partial \kappa_a / \partial r_a$ giving the two terms $\kappa_a / r_a + \partial \kappa_a / \partial r_a$ in Eq. (8). For a cylindrical droplet, L_c does not depend on r_c and $\partial(\kappa_c L_c)/\partial r_c = L_c \partial \kappa_c / \partial r_c$ giving the only term $\partial \kappa_c / \partial r_c$ in Eq. (10).

For both geometries, we suppose the line tension to depend not only on T and μ , but also on the droplet size. This dependence is usually overlooked and, in this case, Eq. (8) transforms into the modified Young equation (2), whereas Eq. (10) transforms into formally classical Young equation (1) (with surface tensions, however, depending on the chemical potential, i.e. on the equilibrium droplet size, that makes the contact angle θ_c different from θ_∞ , see subsection II B).

We suppose the contact line radius (half-width) r to be the only appropriate size variable the line tension can be considered to depend on. It is not clear for the derivation we used in this paper, and some authors suppose the line tension to depend also on the contact angle θ [7, 8], corresponding ‘‘notional’’ derivatives also appear in the work [41]. However, a variational derivation of Eqs. (7), (8), (9), and (10), which considers all three variables R , r , and θ to be independent in some sense, gives an argument in favor of r as the mathematically appropriate size variable for κ in both geometries [24].

Simple dropping the size-dependent term $\partial \kappa / \partial r$ in the generalized Young equations (8) and (10) make them inexact (even if κ is supposed to depend on the droplet size). It can be seen in a model system if the line tension is calculated directly [21]. Also, the generalized Young equation is the simplest way to calculate $\partial \kappa / \partial r$ if θ and r are found and the surface and line tensions (the latter for axisymmetric droplet only) are calculated directly [21].

B. Size dependence of contact angle and relations between pressures, surface tensions, droplet size and chemical potential

Comparing the generalized Young equation (8) or (10) with the classical Young equation (1), one should take into account that these two equations are written for droplets corresponding to *different* values of the chemical potential μ . The classical Young equation corresponds to a macroscopically large (strictly speaking, infinite) drop, i.e. liquid–gas bulk phase coexistence at the binodal. Let us mark the values of the quantities corresponding to the binodal with subscript ‘‘ ∞ ’’. The surface tensions at the binodal then should be denoted as $\sigma_\infty^{\alpha\beta}$, $\sigma_\infty^{\alpha\gamma}$, and $\sigma_\infty^{\beta\gamma}$, and the classical Young equation (1) should be rewritten as

$$\sigma_\infty^{\alpha\beta} \cos \theta_\infty = \sigma_\infty^{\beta\gamma} - \sigma_\infty^{\alpha\gamma}. \quad (11)$$

Subtracting the generalized Young equations (8) and (10) from Eq. (11) we obtain, for an axisymmetric droplet,

$$\sigma_\infty^{\alpha\beta} \cos \theta_\infty - \sigma_a^{\alpha\beta} \cos \theta_a = \delta \Delta \sigma^\gamma + \frac{\kappa_a}{r_a} + \frac{\partial \kappa_a}{\partial r} \quad (12)$$

and a similar equation for a cylindrical droplet:

$$\sigma_{\infty}^{\alpha\beta} \cos \theta_{\infty} - \sigma_c^{\alpha\beta} \cos \theta_c = \delta \Delta \sigma^{\gamma} + \frac{\partial \kappa_c}{\partial r_c}. \quad (13)$$

Here $\delta \Delta \sigma^{\gamma} \equiv \Delta \sigma^{\gamma} - \Delta \sigma_{\infty}^{\gamma}$ with $\Delta \sigma^{\gamma} \equiv \sigma^{\alpha\gamma} - \sigma^{\beta\gamma}$ and $\Delta \sigma_{\infty}^{\gamma} \equiv \sigma_{\infty}^{\alpha\gamma} - \sigma_{\infty}^{\beta\gamma}$. To make these equations more similar to Eq. (3), let us introduce $\delta \sigma_{a,c}^{\alpha\beta} \equiv \sigma_{a,c}^{\alpha\beta} - \sigma_{\infty}^{\alpha\beta}$. Then, Eqs. (12) and (13) can be rewritten as

$$\sigma_{\infty}^{\alpha\beta} (\cos \theta_{\infty} - \cos \theta_a) = \delta \Delta \sigma^{\gamma} + \delta \sigma_a^{\alpha\beta} \cos \theta_a + \frac{\kappa_a}{r_a} + \frac{\partial \kappa_a}{\partial r_a}, \quad (14)$$

$$\sigma_{\infty}^{\alpha\beta} (\cos \theta_{\infty} - \cos \theta_c) = \delta \Delta \sigma^{\gamma} + \delta \sigma_c^{\alpha\beta} \cos \theta_c + \frac{\partial \kappa_c}{\partial r_c}. \quad (15)$$

Now we see, that, in the exact counterpart of Eq. (3) for the difference $\cos \theta_{\infty} - \cos \theta$, we have 4 terms for an axisymmetric droplet (instead of 1) and 3 terms for a cylindrical droplet (instead of 0). How do they depend on the droplet size [the radius (half-width) of the droplet on the substrate]?

For the $\alpha\beta$ liquid–gas interface, let us write down the isothermal Gibbs adsorption equations:

$$d\sigma_{a,c}^{\alpha\beta} = -\Gamma_{a,c}^{\alpha\beta} d\mu, \quad (16)$$

where $\Gamma^{\alpha\beta}$ is the adsorption (the surface excess of matter per unit surface area) at the $\alpha\beta$ interface for corresponding geometry. Since the surface of tension is chosen as the dividing surface in both geometries, these equations do not contain $(\partial \sigma^{\alpha\beta} / \partial R) dR$ terms.

For each of the solid–fluid interfaces, similar equations can be written. Generally, they are more complicated (see, e.g., Sec. 6.3 in [8] and Sec. 3.4.3 in [3]), but in some simple cases (e.g., for non-deformable substrate and such a choice of the solid–fluid dividing surfaces that the amounts of matter of the immobile component of solid do not change in the solid phase at any change of μ) they take [21, 24] the same simple form as (16), so we can write down

$$d\Delta \sigma^{\gamma} \equiv d(\sigma^{\alpha\gamma} - \sigma^{\beta\gamma}) = (\Gamma^{\beta\gamma} - \Gamma^{\alpha\gamma}) d\mu. \quad (17)$$

Integrating Eqs. (16) and (17) from the value μ_{∞} at the binodal to the current value of μ , we obtain, introducing $\delta \mu \equiv \mu - \mu_{\infty}$,

$$\delta \sigma_{a,c}^{\alpha\beta} = -\int_{\mu_{\infty}}^{\mu} \Gamma_{a,c}^{\alpha\beta}(\mu') d\mu' \simeq -\Gamma_{\infty}^{\alpha\beta} \delta \mu, \quad (18)$$

$$\delta \Delta \sigma^{\gamma} = \int_{\mu_{\infty}}^{\mu} (\Gamma^{\beta\gamma} - \Gamma^{\alpha\gamma}) d\mu' \simeq (\Gamma_{\infty}^{\beta\gamma} - \Gamma_{\infty}^{\alpha\gamma}) \delta \mu. \quad (19)$$

Since $\Gamma_a^{\alpha\beta}(\mu_{\infty}) = \Gamma_c^{\alpha\beta}(\mu_{\infty}) = \Gamma_{\infty}^{\alpha\beta}$, the asymptotic expression in (18) is the same for spherical and cylindrical surfaces at the same value of μ , but the exact integral is generally not if $\Gamma_a^{\alpha\beta}(\mu) \neq \Gamma_c^{\alpha\beta}(\mu)$. Thus, $\sigma_a^{\alpha\beta}$ and $\sigma_c^{\alpha\beta}$ generally differ, but at least in the second order in $\delta \mu$:

$$\sigma_a^{\alpha\beta} - \sigma_c^{\alpha\beta} = \delta \sigma_a^{\alpha\beta} - \delta \sigma_c^{\alpha\beta} = O((\delta \mu)^2). \quad (20)$$

The last asymptotic expressions in Eqs. (18) and (19) are valid for small values of $\delta \mu$. How is this quantity related

to the droplet size? This can be estimated using the Laplace equation (7) or (9) for the axisymmetric or cylindrical droplet, respectively. Applying the isothermal Gibbs–Duhem equations $dp = n d\mu$ to liquid and gaseous phases, respectively, we obtain $p^{\alpha} - p^{\beta} \simeq n_{\infty}^{\alpha} \delta \mu$ with n^{α} the number density of molecules in α liquid phase. Here we have neglected the compressibility of the liquid ($n^{\alpha} \simeq n_{\infty}^{\alpha}$) and the number density of molecules n^{β} in the gas ($n^{\beta} \ll n^{\alpha}$). With use of the Laplace equations (7) and (9), and geometric relation (5), we obtain

$$\frac{2\sigma_a^{\alpha\beta}}{R_a} = \frac{2\sigma_a^{\alpha\beta} \sin \theta_a}{r_a} \simeq n_{\infty}^{\alpha} \delta \mu, \quad (21)$$

$$\frac{\sigma_c^{\alpha\beta}}{R_c} = \frac{\sigma_c^{\alpha\beta} \sin \theta_c}{r_c} \simeq n_{\infty}^{\alpha} \delta \mu. \quad (22)$$

We now see that $\delta \mu \propto 1/R = O(1/r)$, i.e., small values of $\delta \mu$ correspond to large droplets, and $\delta \mu \rightarrow 0$ expectedly corresponds to $R \rightarrow \infty$ and $r \rightarrow \infty$.

Thus, for the correction terms in Eqs. (14) and (15) we have

$$\delta \Delta \sigma^{\gamma} \simeq \frac{2\sigma_a^{\alpha\beta} \sin \theta_a}{n_{\infty}^{\alpha} r_a} (\Gamma_{\infty}^{\beta\gamma} - \Gamma_{\infty}^{\alpha\gamma}) = O(\delta \mu) = O(1/r), \quad (23)$$

$$\delta \sigma_a^{\alpha\beta} \simeq -\frac{2\sigma_a^{\alpha\beta} \Gamma_{\infty}^{\alpha\beta} \sin \theta_a}{n_{\infty}^{\alpha} r_a} = O(\delta \mu) = O(1/r), \quad (24)$$

$$\kappa_a / r_a \simeq \kappa_{\infty} / r_a = O(\delta \mu) = O(1/r), \quad (25)$$

where $\kappa_{\infty} = \kappa_a$ at $\mu = \mu_{\infty}$ ($r_a \rightarrow \infty$) is the line tension of the macroscopic (infinite) droplet, and

$$\delta \Delta \sigma^{\gamma} \simeq \frac{\sigma_c^{\alpha\beta} \sin \theta_c}{n_{\infty}^{\alpha} r_c} (\Gamma_{\infty}^{\beta\gamma} - \Gamma_{\infty}^{\alpha\gamma}) = O(\delta \mu) = O(1/r), \quad (26)$$

$$\delta \sigma_c^{\alpha\beta} \simeq -\frac{\sigma_c^{\alpha\beta} \Gamma_{\infty}^{\alpha\beta} \sin \theta_c}{n_{\infty}^{\alpha} r_c} = O(\delta \mu) = O(1/r). \quad (27)$$

As for the terms $\partial \kappa / \partial r$, it can be shown [3, 21, 24, 40] that they are $O((\delta \mu)^2) = O(1/r^2)$. For sufficiently large droplets, $\sin \theta$ can be approximated with $\sin \theta_{\infty}$, with a relative error $O(1/r)$, that makes Eqs. (23), (24), (26), and (27) valid with $\sin \theta_{a,c}$ replaced by $\sin \theta_{\infty}$. The same applies to $\cos \theta_{a,c}$ in the correction terms $\delta \sigma^{\alpha\beta} \cos \theta$ in Eqs. (14) and (15).

Taking this into account, we can now write down the linear in $1/r$ approximations for Eq. (14) and (15):

$$\cos \theta_{\infty} - \cos \theta_a \simeq \frac{\varkappa_a}{\sigma_{\infty}^{\alpha\beta} r_a}, \quad (28)$$

$$\cos \theta_{\infty} - \cos \theta_c \simeq \frac{\varkappa_c}{\sigma_{\infty}^{\alpha\beta} r_c}, \quad (29)$$

where

$$\varkappa_a \equiv \kappa_{\infty} + \frac{2 \sin \theta_{\infty}}{n_{\infty}^{\alpha}} (\Gamma_{\infty}^{\beta\gamma} - \Gamma_{\infty}^{\alpha\gamma} - \Gamma_{\infty}^{\alpha\beta} \cos \theta_{\infty}) \quad (30)$$

and

$$\varkappa_c \equiv \frac{\sin \theta_{\infty}}{n_{\infty}^{\alpha}} (\Gamma_{\infty}^{\beta\gamma} - \Gamma_{\infty}^{\alpha\gamma} - \Gamma_{\infty}^{\alpha\beta} \cos \theta_{\infty}) \quad (31)$$

are the quantities sometimes called the *apparent line tensions* [20, 22, 26–30] of axisymmetric and cylindrical droplets, respectively (see below).

Eqs. (28) and (30) show that the dependence of $\cos \theta_a$ on $1/r_a$, even in the first order in $1/r_a$, is determined not only by the line tension, but also by the adsorptions at the three interfaces. In fact, Eq. (28) should be treated as Eq. (3) often is. This means that the slope of the graph $\cos \theta_a$ vs $1/r_a$ at $1/r_a \rightarrow 0$ does not give the line tension itself but rather a combination of the line tension, the surface tension of the droplet free surface, adsorptions at the three interfaces, and the macroscopic contact angle. Some authors use the term “apparent line tension” meaning the value of the line tension calculated from the dependence of $\cos \theta$ on $1/r$ (denoted further as $\cos \theta(1/r)$) at $1/r \rightarrow 0$ as if Eq. (3) were the correct linear approximation. Then Eq. (30) gives the value of the apparent line tension of axisymmetric droplets. More interesting, Eqs. (29) and (31) show that, for cylindrical droplets, $\cos \theta_c$ also depends on $1/r_c$ in the first order in $1/r_c$. This has been found in simulations [20, 22] and attributed to size dependence of the surface tension $\sigma^{\alpha\beta}$ expressed using the Tolman length [42] $\delta_T \approx \Gamma_{\infty}^{\alpha\beta}/n_{\infty}^{\alpha}$. As it is seen from Eq. (31), dependences of other surface tensions on the droplet size via the chemical potential could also made their contributions to the apparent line tension of cylindrical droplets.

III. LINE TENSION FROM DUAL-GEOMETRY CONTACT ANGLE DEPENDENCES ON DROPLET SIZE

One can easily notice that the apparent line tension (31) of cylindrical droplets, proportional to the slope of the $\cos \theta_c(1/r_c)$ graph at $1/r_c \rightarrow 0$, is exactly half of the second, adsorption-related, term in the apparent line tension (30) of axisymmetric droplets, proportional to the slope of the $\cos \theta_a(1/r_a)$ graph at $1/r_a \rightarrow 0$. Thus, combining data for dependences $\cos \theta_a(1/r_a)$ and $\cos \theta_c(1/r_c)$, one can determine the line tension of a macroscopic droplet as

$$\kappa_{\infty} = \varkappa_a - 2\varkappa_c. \quad (32)$$

Using this relation, we have calculated the line tension κ_{∞} of a macroscopic droplet from the apparent line tensions \varkappa_a and \varkappa_c of sessile droplets simulated by Kanduč et al. [20, 22] using data from Fig. 2(c) in [22]. As one can see in Fig. 2, the values of κ_{∞} calculated with Eq. (32) are in good agreement with ones obtained in [22] by taking into account Tolman length [42] and “line tension stiffness” [41] corrections. It is clearly seen, that the values of \varkappa_a and \varkappa_c are comparable in these simulations that makes κ_{∞} visibly different from \varkappa_a . In contrast, simulations of Isaiev et al. [18] show very weak dependence of $\cos \theta_c(1/r_c)$ comparing to $\cos \theta_a(1/r_a)$ (see Fig. 4 therein). This corresponds to $\varkappa_c \ll \varkappa_a$ and, thus, $\kappa_{\infty} \approx \varkappa_a$.

Eqs. (28)–(31) suggest another idea. With dual-geometry sessile droplet measurements, it is not necessary to use the classical Young equation at all. Subtracting the generalized Young equation for axisymmetric droplets (8) from the one

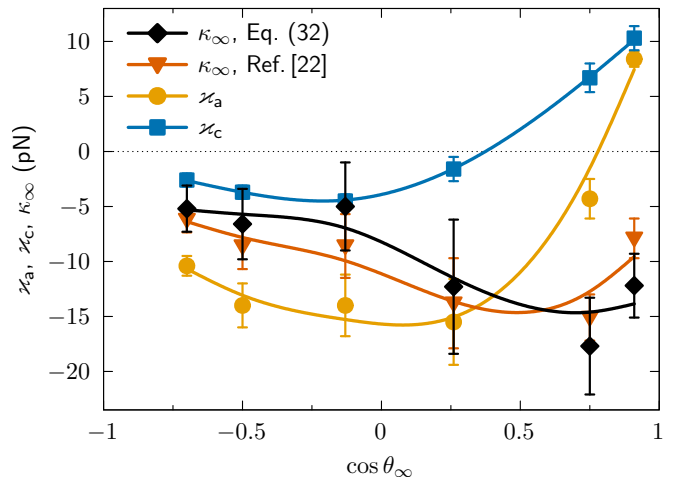


Figure 2. Apparent line tensions of axisymmetric (\varkappa_a) and cylindrical (\varkappa_c) MD-simulated droplets [20, 22] (data taken from Fig. 2(c) in [22]) and corresponding line tension κ_{∞} of macroscopic droplets calculated with Eq. (32) and by the authors of [22] using additional corrections (data taken from Fig. 3 therein) vs the macroscopic contact angle cosine (tuned by surface polarity). An error for κ_{∞} from Eq. (32) is estimated as the sum of an error for \varkappa_a and a doubled error for \varkappa_c . The lines are weighted cubic splines plotted using gnuplot’s [43] `smooth acsplines` method with the weights w/Δ , where Δ is the absolute error of the corresponding value, $w = 500$ pN.

for cylindrical droplets (10) we obtain

$$\sigma_c^{\alpha\beta} \cos \theta_c - \sigma_a^{\alpha\beta} \cos \theta_a = \frac{\kappa_a}{r_a} + \frac{\partial \kappa_a}{\partial r_a} - \frac{\partial \kappa_c}{\partial r_c}. \quad (33)$$

Taking into account Eqs. (24), (27) with subsequent comments and $\partial \kappa / \partial r = O(1/r_a^2)$, the first-order approximation to the combined equation (33) will be

$$\cos \theta_c - \cos \theta_a \simeq \frac{\kappa_{\infty}}{\sigma_{\infty}^{\alpha\beta} r_a}. \quad (34)$$

Here dependences of κ_a on μ and r_a and of $\sigma^{\alpha\beta}$ on μ are no longer taken into account since they give corrections $O(1/r_a^2)$.

All the quantities in Eqs. (33) and (34) must be taken at the same values of the chemical potential and temperature. The chemical potential is often unknown in simulations or measurements. But, according to Eqs. (21) and (22) and taking into account Eq. (20), the same value of $\delta\mu$ corresponds to the relation $R_c \simeq R_a/2$ or, in the same order in $\delta\mu$, to $r_c \simeq r_a/2$. The former relation is expectedly more accurate, since it relies only on the Laplace equations (7) and (9), whereas the latter also uses approximation $\sin \theta_a \simeq \sin \theta_c$.

Thus, to determine the line tension from the measured (in the experiment or modeling) dependences of the $\cos \theta$ on $1/r$ for both axisymmetric and cylindrical droplets at the same conditions, it is sufficient to calculate the difference

$$\cos \theta_c \Big|_{R_c=R_a/2} - \cos \theta_a \Big|_{R_a} \quad \text{or} \quad \cos \theta_c \Big|_{r_c=r_a/2} - \cos \theta_a \Big|_{r_a} \quad (35)$$

and take a linear fit of it vs $1/r_a$ at sufficiently large values of

r_a . The slope of this graph will give $\kappa_\infty/\sigma_\infty^{\alpha\beta}$:

$$\cos \theta_c \Big|_{R_c=R_a/2} - \cos \theta_a \Big|_{R_a} \simeq \frac{\kappa_\infty}{\sigma_\infty^{\alpha\beta} r_a}, \quad (36)$$

$$\cos \theta_c \Big|_{r_c=r_a/2} - \cos \theta_a \Big|_{r_a} \simeq \frac{\kappa_\infty}{\sigma_\infty^{\alpha\beta} r_a}. \quad (37)$$

An additional advantage of this technique is that the graph of the difference $\cos \theta_c - \cos \theta_a$ vs $1/r_a$ must start from a known point (0 at $1/r_a = 0$), thus the slope of the linear graph remains the only fitting parameter. When plotting $\cos \theta_a(1/r_a)$ and $\cos \theta_c(1/r_c)$ independently, each of them must be approximated by a straight line starting from an unknown point $\cos \theta_\infty(0)$, which must be the same for axisymmetric and cylindrical droplets (and this, in principle, should be somehow taken into account to reduce the number of fitting parameters from 4 to 3). Unlike experimental measurements, droplet simulations require more computational resources as the droplet size increases, so approaching droplet sizes whose contact angles is macroscopic can be resource demanding. However, macroscopic contact angle θ_∞ , can be found, e.g., using the classical Young equation (11) and calculating $\sigma_\infty^{\alpha\beta}$ and $\Delta\sigma_\infty^\gamma$ in three simulations of planar interfaces [37].

Experiments with nanosized droplets suggest another possible advantage of using dual-geometry techniques to determine the line tension. For nanosized droplets, the graph $\cos \theta_a$ vs $1/r_a$ can be fairly linear but this linear fit may work well only for small droplets and give a false value of $\cos \theta_\infty$ at extrapolation down to $1/r_a \rightarrow 0$ (see Fig. 5 in [44]) and the slope that does not correspond to asymptotic Eq. (28). In many simulations, the droplets are also nanosized, so the same problem can be with simulated droplets, both axisymmetric and cylindrical, giving false values of \varkappa_a and \varkappa_c . If Eq. (32) is then used, this would ultimately give a wrong value of κ_∞ . However, not only the slope would be wrong in such situation, but, most probably, the extrapolated values of $\cos \theta_\infty$ would be different for $\cos \theta_a$ vs $1/r_a$ and $\cos \theta_c$ vs $1/r_c$ indicating an inconsistency. With use of the technique we proposed, such a situation would appear as a set of points of the quantity (35) vs $1/r_a$ that do not fit a straight line starting from (0,0). Both such indicators would simply mean that the droplets are not large enough for the asymptotic Eqs. (28), (29), and (34) to work and, thus, cannot be used to determine the contact angle θ_∞ and the line tension κ_∞ of macroscopic droplets.

IV. OVERVIEW OF RESULTS AND DISCUSSION

Thermodynamic analysis we have performed shows that droplet size corrections to the contact angle cosine for axisymmetric sessile droplets attributed often to the line tension only, are determined generally by the line tension κ_a , its dependence on the droplet size (directly on the droplet radius r_a on the surface and via the chemical potential) and also by dependences of all three surface tensions on the droplet size (via the chemical potential). The same applies to corrections to the contact angle cosine for cylindrical sessile droplets, except

for the line tension term κ_c/r_c that is absent in the generalized Young equation (10) for cylindrical droplets.

In the first order in $1/r_a$ (28), this gives the slope of $\cos \theta_a$ vs $1/r_a$ to be proportional not to the line tension κ_∞ of macroscopic droplets [as it is widely believed according to Eq. (3)] but rather to the so called ‘‘apparent line tension’’ \varkappa_a , a sum of this line tension κ_∞ and a combination of adsorptions at the three interfaces, the number density of molecules in the liquid phase and the macroscopic contact angle (30).

For cylindrical droplets, the contact angle does also depend on the droplet half-width r_c on the surface already in the first order in $1/r_c$ (29), giving the apparent line tension \varkappa_c . It is determined by the same combination of the adsorptions, the number density of molecules in the liquid phase and the macroscopic contact angle (31) but lacks the numerical coefficient 2 compared to the axisymmetric case (30).

This gives a possibility to determine the line tension κ_∞ from \varkappa_a and \varkappa_c found in dual-geometry measurements (e.g., for droplets simulated at the same conditions, i.e. at the same temperature with the same interaction potentials, etc.) as (32). It was illustrated with calculations of κ_∞ from \varkappa_a and \varkappa_c of MD-simulated droplets [20, 22] (see Fig. 2).

We have also proposed a technique for dual-geometry measurements based on calculation of the slope of the difference $\cos \theta_c - \cos \theta_a$ at the same value of the chemical potential vs $1/r_a$. It can be implemented as a calculation of this difference (35) at $R_c = R_a/2$ or $r_c = r_a/2$. The slope will equal $\kappa_\infty/\sigma_\infty^{\alpha\gamma}$ with $\sigma_\infty^{\alpha\gamma}$ the surface tension of the planar liquid–gas interface. This technique has some advantages discussed in section III.

The Laplace and the generalized Young equations in both geometries, as well as the Gibbs adsorption equation (16) for the liquid–gas interface, were obtained and considered for the surface of tension as the liquid–gas dividing surface. At an arbitrary choice of this dividing surface, all these equations are more complicated [40, 41]. Even though most researchers use these equations in their simple forms, the real choice of the dividing surface is often different or even not specified explicitly. In simulations, it can be done, e.g., by a boundary detection algorithm, and different algorithms can give [45] visibly different dependences of $\cos \theta$ vs $1/r$. This can be considered as an additional source of errors that need to be estimated.

As for the solid–liquid dividing surfaces, we have used the analogue of the Gibbs adsorption equation (17) for the difference $\Delta\sigma^\gamma \equiv \Delta\sigma^\gamma - \Delta\sigma_\infty^\gamma$ written under some conditions that are not necessarily met at an arbitrary choice of these dividing surfaces. However, if the same choice is made in both geometries, these quantities will still cancel, both with use of Eq. (32) and in the proposed technique where Eq. (33) will remain valid. In contrast, the line tensions κ_a and κ_c (including their macroscopic value κ_∞) do generally depend on the choice of the solid–fluid dividing surfaces. For any specific choice, the dual-geometry approach should work, giving the value corresponding to chosen dividing surfaces.

Finally, let us discuss if the proposed technique can be easily adapted to determine the *size-dependent* line tension κ_a and/or κ_c (not only their limit κ_∞ at $r \rightarrow \infty$). Eq. (33) does not contain solid–fluid surface tensions, but it contains the surface tensions $\sigma_{a,c}^{\alpha\beta}$. They can be calculated separately for

free spherical/cylindrical droplets of the same radius $R_{a,c}$ of the liquid–gas surface as for the sessile droplet of the same type of geometry (thus, at the same value of chemical potential). However, since $\kappa_a(\mu, r_a)$ and $\kappa_c(\mu, r_c)$ are different functions, the expression $\partial\kappa_a/\partial r_a - \partial\kappa_c/\partial r_c$ on the right hand side of Eq. (33) is still $O((\delta\mu)^2) = O(1/r_a^2)$ and, therefore, cannot be neglected even in the second order in $1/r_a$. Thus, Eq. (33) can hardly be used to obtain more detailed information on the line tension from dual-geometry measurements of $\cos\theta(1/r)$.

ACKNOWLEDGMENTS

The authors thank N. A. Volkov and M. S. Polovinkin for valuable discussions and comments on the manuscript. The research has been carried out with financial support of the Russian Science Foundation, grant no. 22-13-00151, <https://rscf.ru/en/project/22-13-00151/>

-
- [1] T. Young, III. An essay on the cohesion of fluids, *Phil. Trans. R. Soc. London* **95**, 65 (1805).
- [2] A. I. Rusanov, Classification of line tension, *Colloids Surf. A* **156**, 315 (1999).
- [3] A. I. Rusanov, Surface thermodynamics revisited, *Surf. Sci. Rep.* **58**, 111 (2005).
- [4] V. S. Veselovskii and V. N. Pertsov, Adhesion of bubbles to solid surfaces, *Zh. Fiz. Khim.* **8**, 245 (1936).
- [5] L. M. Shcherbakov and P. P. Ryazantsev, The effect of the energy of the wetting perimeter on the boundary conditions, in *Research in Surface Forces*, Vol. 2. Three-Dimensional Aspects of Surface Forces, edited by B. V. Deryagin (Consultants Bureau, New York, 1966) pp. 33–35.
- [6] B. A. Pethica, Contact angles, *Rep. Prog. Appl. Chem.* **46**, 14 (1961); The contact angle equilibrium, *J. Colloid Interface Sci.* **62**, 567 (1977).
- [7] A. I. Rusanov, On the wetting theory of elastically deformable bodies. 5. Reducing the deformation effects to linear tension, *Colloid J. USSR* **39**, 618 (1977).
- [8] A. I. Rusanov, Thermodynamics of solid surfaces, *Surf. Sci. Rep.* **29**, 173 (1996).
- [9] L. Boruvka and A. W. Neumann, Generalization of the classical theory of capillarity, *J. Chem. Phys.* **66**, 5464 (1977).
- [10] B. M. Law, S. P. McBride, J. Y. Wang, H. S. Wi, G. Paneru, S. Betelu, B. Ushijima, Y. Takata, B. Flanders, F. Bresme, H. Matsubara, T. Takiue, and M. Aratono, Line tension and its influence on droplets and particles at surfaces, *Progr. Surf. Sci.* **92**, 1 (2017).
- [11] F. Bresme and N. Quirke, Computer simulation study of the wetting behavior and line tensions of nanometer size particulates at a liquid-vapor interface, *Phys. Rev. Lett.* **80**, 3791 (1998).
- [12] A. I. Milchev and A. A. Milchev, Wetting behavior of nanodroplets: The limits of Young’s rule validity, *Europhys. Lett.* **56**, 695 (2001).
- [13] H. K. Guo and H.-P. Fang, Drop size dependence of the contact angle of nanodroplets, *Chin. Phys. Lett.* **22**, 787 (2005).
- [14] G. Scocchi, D. Sergi, C. D’Angelo, and A. Ortona, Wetting and contact-line effects for spherical and cylindrical droplets on graphene layers: A comparative molecular-dynamics investigation, *Phys. Rev. E* **84**, 061602 (2011).
- [15] J. H. Weijers, A. Marchand, B. Andreotti, D. Lohse, and J. H. Snoeijer, Origin of line tension for a Lennard-Jones nanodroplet, *Phys. Fluids* **23**, 022001 (2011).
- [16] M. Barisik and A. Beskok, Wetting characterisation of silicon (1,0,0) surface, *Mol. Simul.* **39**, 700 (2013).
- [17] H. Peng, G. R. Birkett, and A. V. Nguyen, The impact of line tension on the contact angle of nanodroplets, *Mol. Simul.* **40**, 934 (2014).
- [18] M. Isaiev, S. Burian, L. Bulavin, M. Gradeck, F. Lemoine, and K. Termentzidis, Efficient tuning of potential parameters for liquid–solid interactions, *Mol. Simul.* **42**, 910 (2016).
- [19] M. Khalkhali, N. Kazemi, H. Zhang, and Q. Liu, Wetting at the nanoscale: A molecular dynamics study, *J. Chem. Phys.* **146**, 114704 (2017).
- [20] M. Kanduč, Going beyond the standard line tension: Size-dependent contact angles of water nanodroplets, *J. Chem. Phys.* **147**, 174701 (2017).
- [21] D. V. Tatyatenko and A. K. Shchekin, Comparable effects of adsorption and line tension on contact angle of a nucleated droplet on a partially wettable substrate, *Interfacial Phenom. Heat Transfer* **5**, 113 (2017).
- [22] M. Kanduč, L. Eixeres, S. Liese, and R. R. Netz, Generalized line tension of water nanodroplets, *Phys. Rev. E* **98**, 032804 (2018).
- [23] S. K. Das, S. A. Egorov, P. Virnau, D. Winter, and K. Binder, Do the contact angle and line tension of surface-attached droplets depend on the radius of curvature?, *J. Phys.: Condens. Matter* **30**, 255001 (2018).
- [24] D. V. Tatyatenko and A. K. Shchekin, Thermodynamic analysis of adsorption and line-tension contributions to contact angles of small sessile droplets, *Colloid J.* **81**, 455 (2019).
- [25] C. A. Ward and J. Wu, Effect of contact line curvature on solid–fluid surface tensions without line tension, *Phys. Rev. Lett.* **100**, 256103 (2008).
- [26] J. Zhang, P. Wang, M. K. Borg, J. M. Reese, and D. Wen, A critical assessment of the line tension determined by the modified Young’s equation, *Phys. Fluids* **30**, 082003 (2018).
- [27] M. Iwamatsu, A generalized Young’s equation to bridge a gap between the experimentally measured and the theoretically calculated line tensions, *J. Adhesion Sci. Technol.* **32**, 2305 (2018).
- [28] B. Zhao, S. Luo, E. Bonaccorso, G. K. Auernhammer, X. Deng, Z. Li, and L. Chen, Resolving the apparent line tension of sessile droplets and understanding its sign change at a critical wetting angle, *Phys. Rev. Lett.* **123**, 094501 (2019).
- [29] N. Kubochkin and T. Gambaryan-Roisman, Wetting at nanoscale: Effect of surface forces and droplet size, *Phys. Rev. E* **98**, 032804 (2018).
- [30] W. Klauser, F. T. von Kleist-Retzow, and S. Fatikow, Line tension and drop size dependence of contact angle at the nanoscale, *Nanomaterials* **12**, 369 (2022).
- [31] L. Schimmele and S. Dietrich, Line tension and the shape of nanodroplets, *Eur. Phys. J. E* **30**, 427 (2009).
- [32] S. M. Dammer and D. Lohse, Gas enrichment at liquid-wall interfaces, *Phys. Rev. Lett.* **96**, 206101 (2006).
- [33] F. Ould-Kaddour and D. Levesque, Molecular simulation of fluid–solid interfaces at nanoscale, *J. Chem. Phys.* **135**, 224705 (2011).
- [34] H. Jiang, F. Müller-Plathe, and A. Z. Panagiotopoulos, Contact

- angles from Young's equation in molecular dynamics simulations, *J. Chem. Phys.* **147**, 084708 (2017).
- [35] M. Kanduč and R. R. Netz, Atomistic simulations of wetting properties and water films on hydrophilic surfaces, *J. Chem. Phys.* **146**, 164705 (2017).
- [36] M. Isaiev, S. Burian, L. Bulavin, W. Chaze, M. Gradeck, G. Castanet, S. Merabia, P. Koblinski, and K. Termentzidis, Gibbs adsorption impact on a nanodroplet shape: Modification of Young–Laplace equation, *J. Phys. Chem. B* **122**, 3176 (2018).
- [37] S. R. Carlson, O. Schullian, M. R. Becker, and R. R. Netz, Modeling water interactions with graphene and graphite via force fields consistent with experimental contact angles, *J. Phys. Chem. Lett.* **15**, 6325 (2024).
- [38] S. Mechkov, G. Oshanin, M. Rauscher, M. Brinkmann, A. M. Cazabat, and S. Dietrich, Contact line stability of ridges and drops, *EPL* **80**, 66002 (2007).
- [39] A. I. Rusanov, D. V. Tatyanyenko, and A. K. Shchekin, Comment on “Size dependence of bubble wetting on surfaces: breakdown of contact angle match between small sized bubbles and droplets” by H. Zhang and X. Zhang, *Nanoscale*, 2019, 11, 2823, *Nanoscale* **13**, 4308 (2021).
- [40] A. I. Rusanov, A. K. Shchekin, and D. V. Tatyanyenko, The line tension and the generalized Young equation: the choice of dividing surface, *Colloids Surf. A* **250**, 263 (2004).
- [41] L. Schimmele, M. Napiórkowski, and S. Dietrich, Conceptual aspects of line tensions, *J. Chem. Phys.* **127**, 164715 (2007).
- [42] R. C. Tolman, The effect of droplet size on surface tension, *J. Chem. Phys.* **17**, 333 (1949).
- [43] T. Williams and C. Kelley, gnuplot 6.0. An interactive plotting program, https://gnuplot.sourceforge.net/docs_6.0/Gnuplot_6.pdf (2023).
- [44] L.-O. Heim and E. Bonaccorso, Measurement of line tension on droplets in the submicrometer range, *Langmuir* **29**, 14147 (2013).
- [45] M. S. Polovinkin, N. A. Volkov, D. V. Tatyanyenko, and A. K. Shchekin, Contact angle calculations for argon and water sessile droplets on planar lyophilic and lyophobic surfaces within molecular dynamics modeling, *Colloids Surf. A* [10.1016/j.colsurfa.2024.134932](https://doi.org/10.1016/j.colsurfa.2024.134932) (2024).